

2017

# Computational Fluid Dynamic Modelling of a Small-Scale Vertical Axis Wind Turbine

Ashley Victoria Chase  
*University of Vermont*

Follow this and additional works at: <https://scholarworks.uvm.edu/hcoltheses>

---

## Recommended Citation

Chase, Ashley Victoria, "Computational Fluid Dynamic Modelling of a Small-Scale Vertical Axis Wind Turbine" (2017). *UVM Honors College Senior Theses*. 187.  
<https://scholarworks.uvm.edu/hcoltheses/187>

This Honors College Thesis is brought to you for free and open access by the Undergraduate Theses at ScholarWorks @ UVM. It has been accepted for inclusion in UVM Honors College Senior Theses by an authorized administrator of ScholarWorks @ UVM. For more information, please contact [donna.omalley@uvm.edu](mailto:donna.omalley@uvm.edu).

UNIVERSITY OF VERMONT  
DEPARTMENT OF MECHANICAL ENGINEERING  
UVM HONORS COLLEGE SENIOR THESIS

---

**Computational Fluid Dynamic  
Modelling of a Small-Scale  
Vertical Axis Wind Turbine**

---

*Author:*  
Ashley Chase

*Thesis Advisor:*  
Dr. Ting Tan

May 17, 2017



# Contents

<b>Abstract</b>	<b>2</b>
<b>Nomenclature</b>	<b>3</b>
<b>1 Introduction</b>	<b>4</b>
1.1 Project History and Current Scope . . . . .	4
1.2 Characteristic Equations of Wind Turbines . . . . .	7
1.3 Governing CFD Equations . . . . .	8
<b>2 Modelling Set-Up</b>	<b>9</b>
2.1 Turbulence Modelling . . . . .	9
2.2 Mesh Parameters . . . . .	11
2.3 Initial and Boundary Conditions . . . . .	12
<b>3 Simulation Results</b>	<b>15</b>
3.1 Wind Turbine Efficiency . . . . .	15
3.2 Mesh Convergence and Simulation Validation . . . . .	18
3.3 Post-Simulation Discussion . . . . .	23
<b>4 Conclusions and Future Work</b>	<b>24</b>
<b>5 Acknowledgements</b>	<b>26</b>
<b>References</b>	<b>27</b>
<b>6 Appendices</b>	<b>29</b>
6.1 Exponentially Increasing Power Coefficient Curves . . . . .	29
6.2 Convergence Plots . . . . .	30
6.3 Mesh Attempts . . . . .	31

## **Abstract**

A small scale vertical axis wind turbine with bamboo blades was built at the University of Vermont in 2014. Prior to 2016, the efficiency of the wind turbine was not fully quantified. Thus, it was desirable to estimate the efficiency using computational fluid dynamic models. Thus, a SolidWorks file of the geometry was created and imported into SimScale, a cloud based CFD software, for analysis. Steady-state, quasi 2D simulations of the geometry were simulated with a constant unidirectional wind flow to mimic wind tunnel testing conditions.

Simultaneously, a UVM Senior Design team was completing a physical wind tunnel test of the bamboo wind turbine. From the simulations the VAWT was found to have a range of efficiencies from 0-0.55% at TSR's of 0.06-0.11, while from the wind tunnel test the efficiencies were in the 0-0.13% range for TSR's of 0-0.125. Though the simulations calculate a slightly higher efficiency of the wind turbine than physically obtained data, they provide a good estimate. Because the wind turbine's efficiency is  $< 1\%$ , future work will be done with CFD to test altered geometries for the bamboo VAWT to improve its' performance.

## Nomenclature

$\rho$  = Air density ( $kg/m^3$ )

$F_1$  = Blending Function

$x, y, z$  = Cartesian Coordinates (m)

$u, v, w$  = Cartesian Components of the Velocity vector (m/s)

$D$  = Diameter (m)

$y^+$  = Dimensionless Wall Distance

$\vec{V}$  = Direction Vector (m/s)

$\mu$  = Dynamic Viscosity ( $\frac{kg}{m \cdot s}$ )

$P_k$  = Effective Rate of Production of k ( $\frac{kg}{m \cdot s^3}$ )

$\mu_k$  = Effective Viscosity ( $\frac{kg}{m \cdot s}$ )

$U_\infty$  = Free-Stream Velocity (m/s)

$u_*$  = Friction Velocity (m/s)

$\vec{g}$  = Gravity Vector ( $\frac{m}{s^2}$ )

$\nu$  = Kinematic Viscosity ( $\frac{kg}{m \cdot s}$ )

$P_m$  = Mechanical Power (W)

$P$  = Pressure (Pa)

$\Omega$  = Rotational Speed (rad/s)

$\omega$  = Specific Turbulent Dissipation Rate ( $\frac{1}{s}$ )

$k$  = Specific Turbulent Kinetic Energy ( $\frac{m^2}{s^2}$ )

$t$  = Time (s)

$\lambda$  = Tip Speed Ratio

$T$  = Torque ( $N \cdot m$ )

$I$  = Turbulence Intensity

$\beta^*$  = Turbulence Modelling Constant

$l$  = Turbulent Length Scale (m)

$C_\mu$  = Turbulent Modelling Constant

$R$  = Wind Turbine Radius (m)

# 1 Introduction

## 1.1 Project History and Current Scope

A small-scale vertical axis wind turbine was built during the 2013-2014 academic year by a Student Experience in Engineering Design (SEED) team at the University of Vermont. Vertical axis wind turbines have gained popularity in recent years due to the simplicity of their design. Vertical axis wind turbines accept wind from all directions, thus do not require yawing mechanisms, a key component to horizontal axis wind turbines. They are also smaller and quieter than HAWT's, thus fit better in urban areas where there is not a lot of space or desire for noise pollution.<sup>11</sup> The possibilities for vertical axis wind turbines are vast. They typically have 2 to 5 blades, which come in a wide variety of geometries. Research into VAWT's has even led to the development of similarly shaped hydro-kinetic turbines, which are under investigation to harness the energy of rivers and oceans around the world.

The wind turbine designed at the University of Vermont was built in the Gorlov style with three helical blades. This wind turbine differs from other wind turbines, because it's blades are built from a 3D printed ABS plastic skeleton that has been wrapped in bamboo veneer. The blades are connected to bamboo culms by custom 3D printed parts, which in turn connect to the carbon fiber rotor of the wind turbine. The wind turbine was constructed with the guidance of Dr. Ting Tan and Dr. Tian Xia, professors in the civil engineering and electrical engineering departments, respectively.



Figure 1: VAWT with Bamboo Blades Built and Designed at the University of Vermont

The wind turbine was a component to the “Wind and Solar Powered Street Light” project. The goal of the project was to create a hybrid energy system that could power a streetlamp. The system was to be both sustainable and aesthetically pleasing in a natural setting.

Thus, the idea of using bamboo as a building material instead of the carbon fiber reinforced composites that are typically used in wind turbine blades, came about. Bamboo is a naturally strong and resilient material, having an average tensile strength of 503 MPa.<sup>1</sup> It is also a fast-growing renewable resource, growing a maximum of 35 inches per day. This makes it an incredibly sustainable structural material.

The objective of this thesis is to quantify the power efficiency of the described wind turbine using computational fluid dynamic (CFD) modelling. CFD modelling based on Reynolds-Averaged Navier–Stokes (RANS) equations, has become an effective method of characterizing the efficiency and flow field of vertical and horizontal wind turbines. Advancements in computational power and the ability to characterize complex flows have made CFD modelling an effective and time-efficient means of estimating turbine efficiency. Today, there are

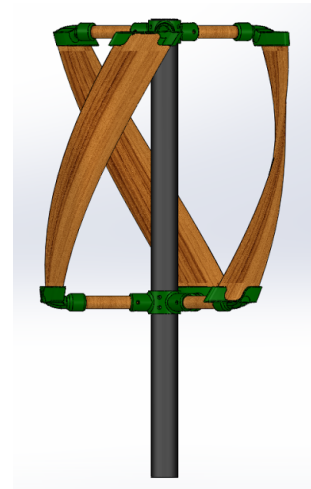


Figure 2: SolidWorks Model of Bamboo VAWT

even free cloud-based simulation softwares, such as SimScale, that make CFD modelling more accessible than ever. Due to its' convenience and affordability, Simscale will be used to analyze the bamboo wind turbine. A Solidworks model of the turbine is shown in Figure 2.

The dimensions of the wind turbine are as follows:

Table 1: Wind Turbine Parameters

Component	Dimension
Airfoil	NACA 0018
Turbine Height	0.588547 m
Turbine Diameter	0.489665 m
Rotor Diameter	0.0508 m
Rotor Length	0.91187 m
Twist Angle	80°
Pitch Angle	0°

It should also be noted that a 2016-2017 UVM SEED team, including myself, has been working this year on the physical wind tunnel testing of this wind turbine. The team designed and built a test frame and testing system that collected the data needed to characterize the efficiency of the wind turbine. The team conducted their initial test at the SOH Wind Engineering wind tunnel facility in Williston VT, on March 7th, 2017. Thus, CFD results can be compared to the real-life testing to prove the model's accuracy.



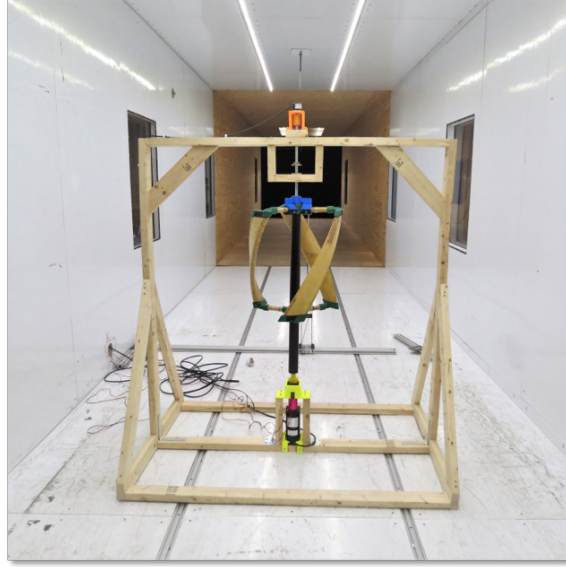


Figure 3: Wind Turbine as SOH Wind

## 1.2 Characteristic Equations of Wind Turbines

The efficiency of a vertical axis wind turbine is characterized by a power coefficient curve, which plots the coefficient of power against the tip speed ratio, given by Equations (1) and (2).

$$\lambda = \frac{\Omega R}{U_\infty} \quad (1)$$

$$C_p = \frac{P_m}{\frac{1}{2}\rho A U_\infty^3} \quad (2)$$

Where  $\omega$  is the rotational speed of the wind turbine,  $R$  is the radius of the wind turbine,  $U_\infty$  is the free-stream velocity of the wind,  $\rho$  is the density of the air,  $A$  is the frontal area of the turbine, and  $P$  is the mechanical power output.

Mechanical power output, the actual power output of the wind turbine found, in this case, though CFD simulation, is given by:

$$P_m = T\Omega \quad (3)$$

Where T is the torque on the wind turbine, which can be found in SimScale by calculating the summation of forces and moments on the blades of the wind turbine.

### 1.3 Governing CFD Equations

As mentioned, the flow through the wind turbine is examined using the Reynold's-Averaged Navier-Stokes equations. The RANS equations are the governing equations for moving fluids. They can be used to calculate how the velocity, pressure, temperature, and density of a fluid flow are related, given that the necessary initial and boundary conditions are known.<sup>17</sup> Due to the low velocities and Mach numbers used in this study, the flow can be considered in-compressible. Thus the defining equations are as follows:<sup>2</sup>

Incompressible continuity equation:

$$\frac{\partial(\rho u)}{\partial x} + \frac{\partial(\rho v)}{\partial y} + \frac{\partial(\rho w)}{\partial z} = 0 \quad (4)$$

Incompressible Navier-Stokes Equation:

$$\rho \frac{D\vec{V}}{Dt} = -\vec{\nabla}P + \rho\vec{g} + \mu\nabla^2\vec{V} \quad (5)$$

Because the properties of fluid flows vary through time, the RANS equations calculate a statistical average to quantify each property. The properties are defined by the Reynold’s Decomposition equation, equation 6, which breaks the property into average and fluctuating components.<sup>3</sup>

$$u(x, t) = \bar{u}(x) + u'(x, t) \quad (6)$$

## 2 Modelling Set-Up

### 2.1 Turbulence Modelling

Choosing the proper turbulence model is a crucial step in starting any CFD simulation. Reynolds-Averaged Navier–Stokes (RANS) based models available include: the k- $\epsilon$ , k- $\omega$  and k- $\omega$  SST (Shear Stress Transport) models. The k- $\omega$  SST is a combination of the k- $\epsilon$  and k- $\omega$  models and has been shown to be the most accurate model for predicting flow separation and providing accurate wind turbine efficiency while being computationally inexpensive.<sup>4,6,7</sup> Using the k- $\omega$  SST model provides two benefits. The first being that it limits shear stress by preventing turbulent shear stress from becoming too large in “adverse pressure gradient regions”. The second benefit

is that this model contains a “production limiter” which prevents the accumulation of turbulence in stagnant regions.<sup>10</sup> The  $k$ - $\omega$  SST model is defined by the following two equations.<sup>12</sup>

The specific turbulent kinetic energy equation:

$$\frac{\partial}{\partial t}(\rho k) + \frac{\partial}{\partial x_i}(U_i \rho k) = \frac{\partial}{\partial x_j}(\mu_k \frac{\partial}{\partial x_j} k) + P_k - \beta^* \rho \omega k \quad (7)$$

The specific turbulent dissipation rate equation:

$$\frac{\partial}{\partial t}(\rho \omega) + \frac{\partial}{\partial x_i}(U_i \rho \omega) = \frac{\partial}{\partial x_j}(\mu_\omega \frac{\partial}{\partial x_j} \omega) + P_\omega - \beta \rho \omega^2 + 2\rho(1 - F_1) \frac{1}{\omega} \frac{1}{\sigma_{\omega,2}} \frac{\partial}{\partial x_j} k \frac{\partial}{\partial x_j} \omega \quad (8)$$

In SimScale, the  $k$ - $\omega$  SST model requires the input of two defining constants, the turbulent kinetic energy term,  $k$ , and the turbulence dissipation rate,  $\omega$ . The turbulent kinetic energy is given by Equation 9.<sup>11</sup>

$$k = \frac{3}{2}(UI)^2 \quad (9)$$

Where  $U$  is the inlet velocity and  $I$  is the turbulence intensity, which is assumed to be between 1-5%, as this is a medium turbulence case.<sup>4</sup>

The specific turbulence dissipation rate is determined by Equation 10.

$$\omega = \frac{\sqrt{k}}{l C_\mu^{1/4}} \quad (10)$$

Where  $l$  is the turbulent length scale, which is defined as  $0.07 \times (\text{Diameter of the Turbine})$  and  $C_\mu$  is a constant, defined as 0.9.<sup>8</sup>

## 2.2 Mesh Parameters

A computer aided design (CAD) model of the wind turbine was imported in SimScale. From there, a mesh was created. The mesh breaks the flow field into a finite number of elements to be individually analyzed by the CFD solver. When creating a mesh it is important to optimize the number of cells created. The higher the number of cells, the better convergence your simulation will have, but also computation time increases with mesh size.

A hex-dominant parametric mesh was created for a quasi-2D slice of the turbine. Though it has been noted that 2D simulations tend to slightly over-estimate the power coefficient of wind turbines, they are often used as an estimate because they require significantly less computational time and power.<sup>9</sup> The mesh used in this study is a rectangular region with three region mesh refinements. Two of these refinements are rectangular in shape, and increase in refinement closer to the turbine and the wake area behind the turbine. The third region refinement is a cylindrical region around the wind turbine itself. An “Inflate Boundary Layer” refinement was

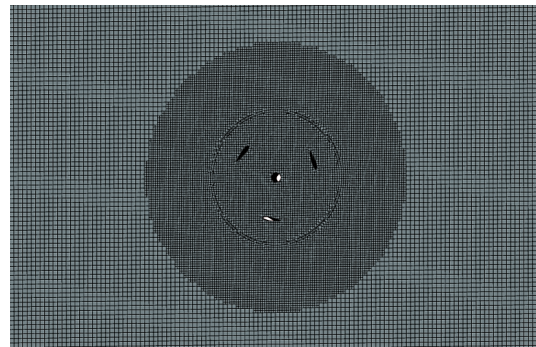


Figure 4: Close Up of Mesh

also used on the wind turbine surfaces, to more accurately depict the boundary layer region. Lastly, a surface refinement is used in order to create a cylindrical rotating “cellZone” around the wind turbine.<sup>12</sup> A zoomed in view of the mesh around the turbine is shown in Figure 4 and the entire mesh is shown in Figure 5.

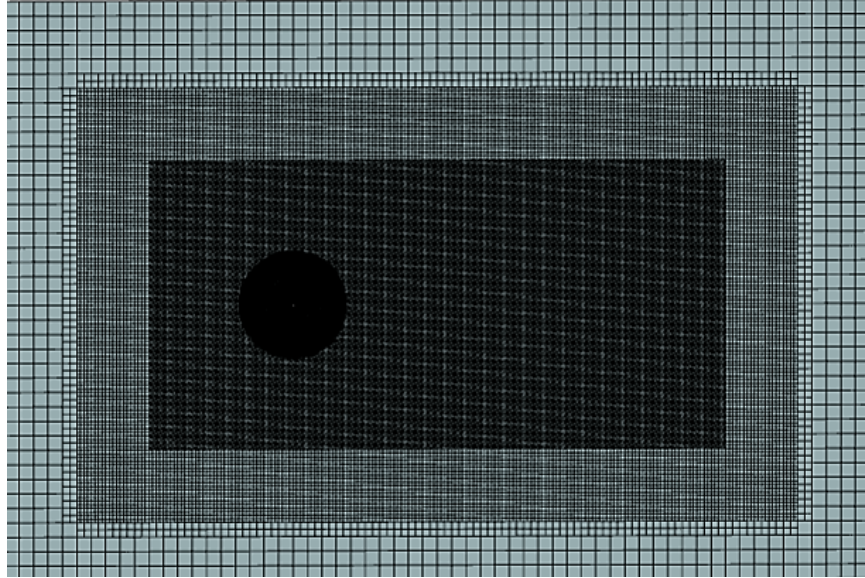


Figure 5: Mesh Refinements

Several meshes were created in the process, three of which are shown in the Appendices, in Figures 22, 23 and 24. However, this mesh resulted in the best convergence.

### 2.3 Initial and Boundary Conditions

Simulations were initially run at a wind speed of 5 m/s with tips speed ratios ranging from 1-8. After the wind tunnel test, however, it was realized that the tip speed ratios for the wind turbine were actually much lower than expected, so new simulations were run at tip speed ratios from 0-1 to create a more accurate picture of

the wind turbine’s characteristics. Wind tunnel test data was only recorded for wind speeds of 9-16 m/s, so for comparison sake, simulations were also run at tip speed ratios from 0-1 at 12 m/s.  $k$  and  $\omega$  values were determined based on Equations (9) and (10).

Table 2: Initial Conditions at 5 and 12 m/s

	5 m/s	12 m/s
Pressure (Pa)	0	0
$k$ ( $m^2s^2$ )	0.00375	0.1994
omega (1/s)	3.375	5.5027

A diagram of the boundary conditions used in the simulations is shown in Figure 6. The mesh is broken up into two sub-meshes. The outer region that simulates the flow of wind in a uni-axial direction, and an inner rotational zone. The rotational zone contains the wind turbine geometry by using the “cellZone” created in the meshing process. This sub-mesh simulates rotational motion at a set radial velocity. SimScale provides two methods for simulating rotational motion: the multi-reference frame method, and the arbitrary mesh interface approach. The multi-reference frame (MRF) method was used in this study, as it is less computational expensive. The MRF is a “Steady-State” approximation of the transient rotating motion at an instance of time.<sup>1312</sup> MRF alters the governing fluid equations to take into account the effects of rotation.

As seen in Figure 6 there is a velocity inlet of either 5 or 12 m/s, a 0 Pa pressure

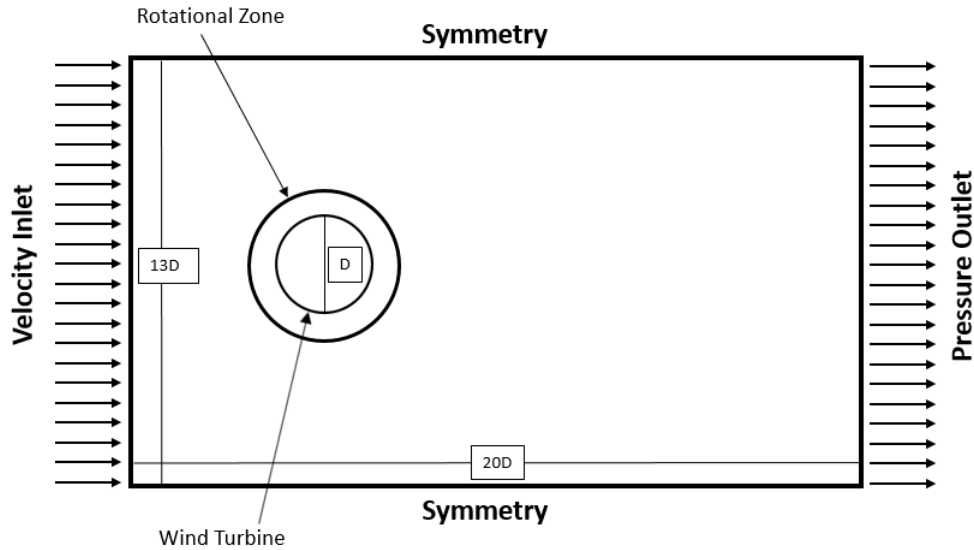


Figure 6: Geometry of Computational Domain

outlet, and a symmetry condition on either side. Not shown is the additional non-slip condition applied to the blades of the wind turbine. Figure 6 also displays the dimensions of the solution field, in terms of the diameter of the wind turbine ( $D$ ).

Two result control items were also added to every simulation. The first is a “Forces and Moments” control, which is used to calculate the torque generated on the wind turbine blades. This generates a force plot in the post-processor that displays the forces and moments in the  $x, y$ , and  $z$  directions as a function of time. The pressure moment around the center of the wind turbine is used to determine power output, as described by Equation (3).

The second result control item used was the “Turbulence” item, which calculates the dimensionless wall distance ( $y^+$ ), which is used to determine whether the mesh used has a high enough resolution near the walls of the geometry. The dimensionless



wall distance,  $y_+$ , is defined by equation 11:

$$y_+ = \frac{u_* y}{\nu} \quad (11)$$

Where  $u_*$  is the friction velocity,  $y$  is the distance to the nearest wall, and  $\nu$  is the kinematic velocity.<sup>14</sup> After simulations, if the  $y_+$  value is too high, the mesh must be refined to have smaller finite elements near the wall. In the case of simple and stationary geometries, it is ideal to have  $y_+$  values close to 1. However, because of the complexity of the geometry and the rotational motion used in this study,  $y_+$  values are aimed to be under 100.

## 3 Simulation Results

### 3.1 Wind Turbine Efficiency

Once the simulations were set-up, multiple runs were done at various tip speed ratios. The tip speed ratio is easily changed in each simulation by changing the rotational velocity of the rotating zone. Power coefficient curves were created for 5 and 12 m/s, as shown in Figures 7 and 8.

As shown, the efficiency ranges from 0-0.03% for tip speed ratios of 0-0.1 for 5 m/s and efficiencies of 0-0.27% for tip speed ratios of 0.06-0.11 at 12 m/s. The corresponding power outputs to these tip speed ratios are shown in Table 3.

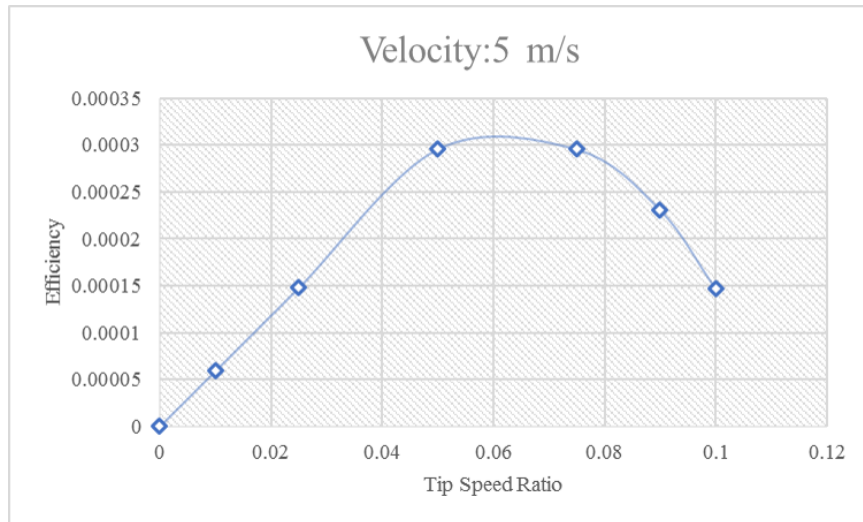


Figure 7: Power Coefficient Plot, V=5 m/s

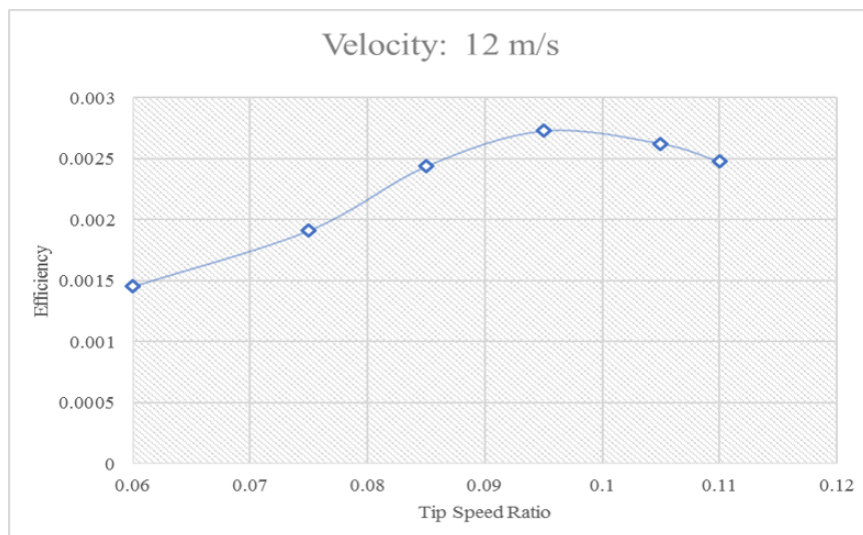


Figure 8: Power Coefficient Plot, V=12 m/s

The 12 m/s plot can be validated by comparing it to that of the real data collected during the wind tunnel test. This data is shown in Figure 9.

The tip speed ratios at 12 m/s are very similar when comparing simulation and real data. The efficiencies are slightly lower from the wind tunnel data, however. They are between 0-0.13%. This could be accounted for in a few ways. First, added resistance

Table 3: Power Outputs

<b>Power Output vs. TSR</b>			
<b>5 m/s</b>		<b>12 m/s</b>	
TSR	Power Output (W)	TSR	Power Output (W)
0.01	0.005746142	0.06	0.238656375
0.025	0.014365355	0.075	0.3138646
0.05	0.028723711	0.085	0.399998762
0.075	0.028716712	0.095	0.447696449
0.09	0.022449848	0.105	0.430586937
0.1	0.014276468	0.11	0.406723977

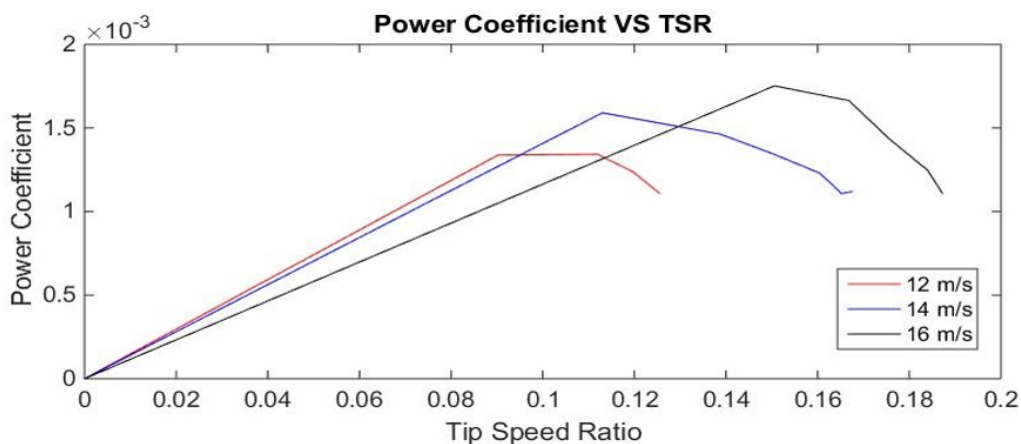


Figure 9: Wind Tunnel Test Power Coefficient Plot

was added to the test system by the testing equipment. Second, the blades of the wind turbine had attached LEDs and the bamboo blade surface was fairly rough. Both of these things are not accounted for in the simulations and likely lowered the efficiency of the actual turbine. 2D simulations are also known for slightly overestimating the efficiency of VAWTs, as mentioned previously.<sup>15</sup>

Both sets of data, from experimentation and simulation, show the wind turbine having very low efficiency. Thus, work has begun to determine ways of improving efficiency. One measure has been to explore different possible pitch angles for the

blades. The current turbine has a pitch angle of  $0^\circ$ . Some studies suggested that a  $-2^\circ$  pitch angle could improve efficiency. Thus, the SolidWorks model of the wind turbine was altered and simulations were run to compare efficiency. Simulations were run with the same mesh, at a wind speed of 9 m/s, as that was experimentally determined to be the start-up wind speed for the turbine. The results are displayed in Table 4.

Table 4: Change in Efficiency and Power Output with Change in Pitch Angle

TSR	Pitch Angle = 0		Pitch Angle = -2	
	Efficiency (%)	Power Output (W)	Efficiency (%)	Power Output (W)
<b>0.1</b>	0.257900007	0.356923293	0.566695099	0.784130341
<b>0.15</b>	0.38689646	0.535344763	0.849222935	1.175061283
<b>0.2</b>	0.515326401	0.713051988	1.132661564	1.567252479
<b>0.25</b>	0.642973971	0.889676654	1.417375302	1.961208031
<b>0.3</b>	0.769437511	1.064870738	1.703145559	2.357085328
<b>0.4</b>	1.018630341	1.409743647	2.267771337	3.13850482
<b>0.5</b>	1.256893662	1.739490552	2.867174817	3.968055259

As seen, there is a slight change in efficiency and power output for each respective tip speed ratio at the  $-2^\circ$  pitch angle, however not a drastic difference. The efficiencies are still much lower than desirable. More simulations will need to be run with various wind turbine geometries to continue optimizing efficiency.

### 3.2 Mesh Convergence and Simulation Validation

The simulation can be validated in many ways. The first is generally by looking at the solution field to see if it looks accurate. Visualization of the flow field around the wind turbine was created using ParaView. Visualization was created of a 12 m/s

wind speed simulation at a 0.12 tip speed ratio and of a 5 m/s simulation at a 0.15 tip speed ratio. These images can be seen in Figures 10 and 11.

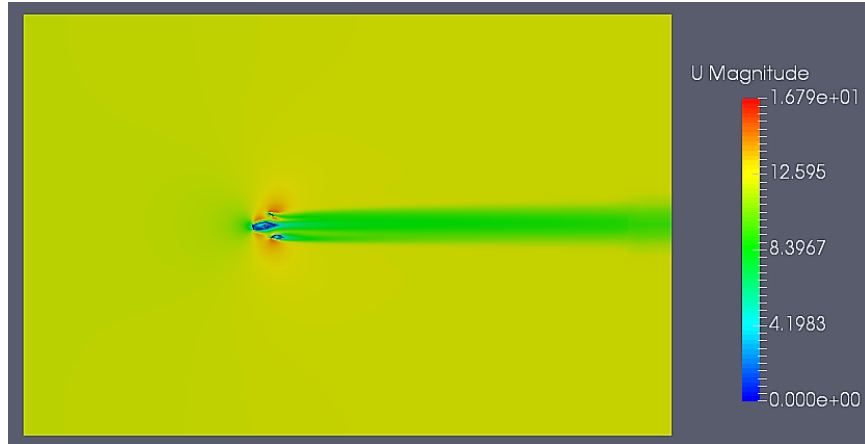


Figure 10: Solution Field of Velocity, for 12 m/s

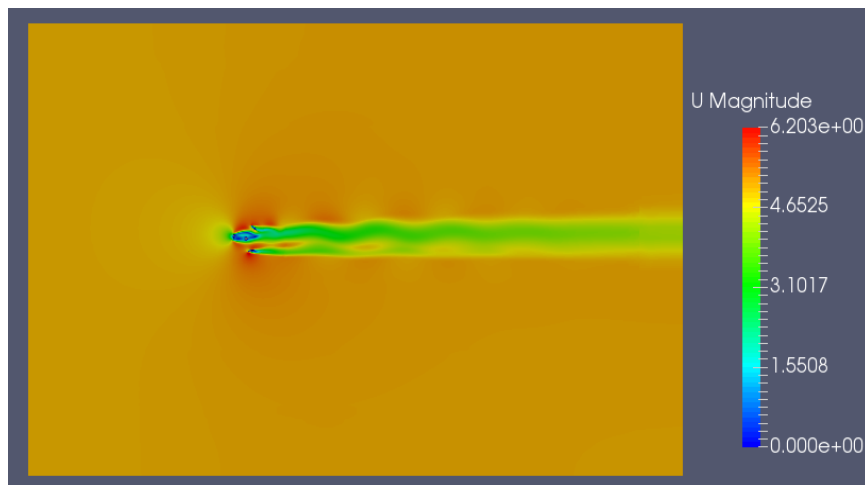


Figure 11: Solution Field of Velocity, for 5 m/s

From this solution field it can be seen that the simulation has accurately defined the stagnation points of the flow at the turbine surfaces, as the velocity drops to 0. Throughout the majority of the solution field the velocity is approximately 5 or 12 m/s as it should be. Also, the velocity on the the right side of the turbine drops, due

to some of the winds energy being transferred to the wind turbine.

Vorticity streamline plots were also created of the solution fields. Close ups of these images are shown in Figure 12.

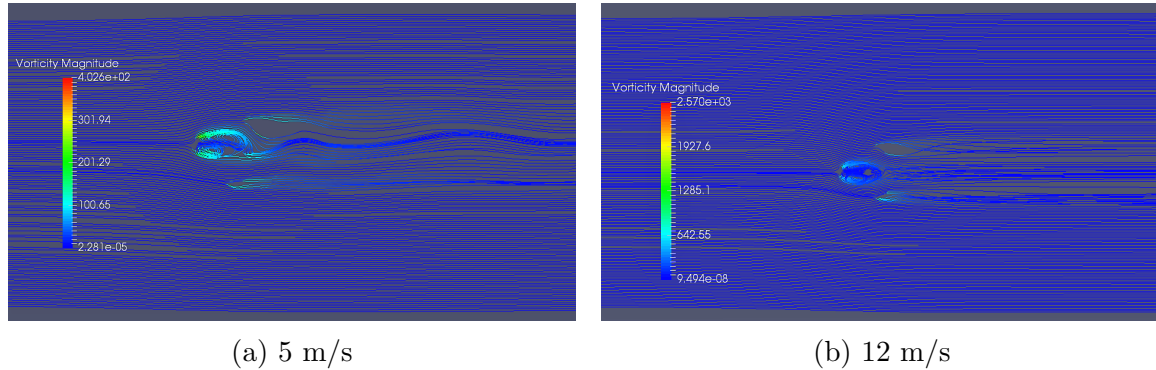


Figure 12: Vorticity Streamlines

As seen, the areas of highest vorticity occur around the blades and rotor of the wind turbine.

After initially taking a look at the solution fields, more sophisticated methods of validation are used. The next step is to check the convergence plots created in the post-processor. These plot the convergence of the CFD solvers results over the runtime of the simulation. Ideally, the user would like this convergence to approach as closely to zero as possible. In most cases convergence of  $10^{-4}$  -  $10^{-5}$  is considered acceptable. Examples of convergence plots from both the 5 m/s and 12 m/s simulations are shown in Figures 13 and 14.

These convergence plots are from low tip speed ratio simulations, used in the Power Coefficient plots. As can be seen the convergence values were found to be between  $10^{-4}$  -  $10^{-6}$ . However, for the same mesh at higher tip speed ratio, the convergence

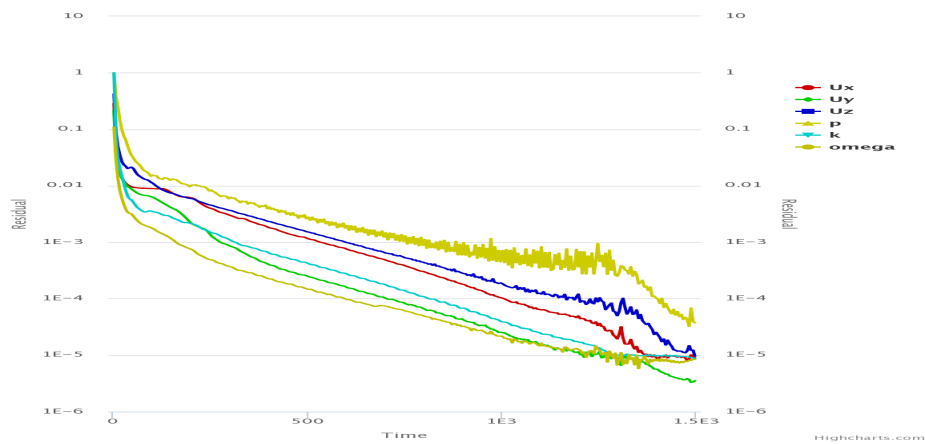


Figure 13: Convergence Plot, 5 m/s

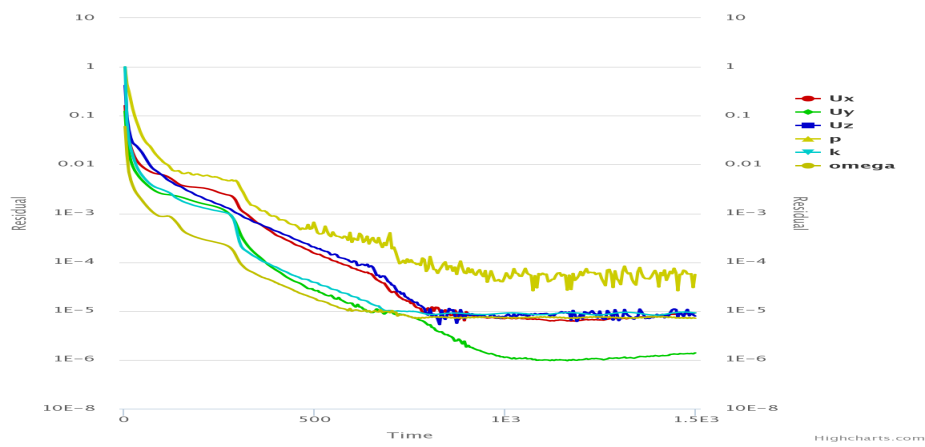


Figure 14: Convergence Plot, 12 m/s

values were between  $10^{-2}$  -  $10^{-5}$ . Examples of convergence plots for 5 m/s at tip speed ratios of 3 and 4 can be seen in Figures 20 and 21 in the Appendices. Since the power coefficient curves only run at lower tip speed ratios, this was not considered a problem.

The  $y^+$  values for the 5 m/s simulations were found to be in the range of 70-80, varying slightly with change in tip speed ratio. The 12 m/s runs had  $y^+$  values in the 100-150 range, which was slightly higher than desirable, but since these simulations

were run at such a high wind velocity, it was difficult to lower that number any further. A plot of the  $y^+$  solution field for 5 m/s is shown in Figure 15.



Figure 15: Example Y Plus Solution Field, 5 m/s

As seen, the majority of the solution field is zero. Zooming in on the wind turbine itself, it can be seen that the highest  $y^+$  values are found on the surface of the blades. This can be seen in Figure 16.



Figure 16: Example Y Plus Solution Field, Zoomed-In

This is expected as the highest levels of turbulence and flow separation occur on the blade surfaces.

Grid convergence was studied at 12 m/s and a tips speed ratio of 0.075, 0.095, and



0.11. The convergence of efficiency calculations was looked at for the original mesh, a courser mesh, and a finer mesh. These results are presented in Table 5.

<b>Efficiency Mesh Convergence, 12 m/s</b>				
		<b>Orginal</b>	<b>Course</b>	<b>Fine</b>
TSR:0.075	Efficiency	0.001921	0.001884	0.001789
	% decrease/ increase	-----	1.9384	-6.87076
TSR:0.095	Efficiency	0.002729	0.002487	0.00258
	% decrease/ increase	-----	-8.898	-5.49215
TSR:0.11	Efficiency	0.002403	0.002515	0.002188
	% decrease/ increase	-----	4.643527	-8.95872

Table 5: Percent Increase/Decrease for Mesh Convergence Study

As seen, the power coefficient curves have relatively small changes between meshes, with less than 10% increase or decrease between them. This shows grid convergence when varying the number of finite elements used during simulation.

### 3.3 Post-Simulation Discussion

A problem I encountered while obtaining these results was that to set-up the simulations in SimScale, the user has to define an input velocity and a rotating speed for the rotational zone, thus by Equation 1, defining a set tip speed ratio for every simulation run. My issue with this, is that there is no way to pre-determine the tip speed ratio that a specific wind turbine will operate at.

Available literature on vertical axis wind turbines showed that most ran at TSR's of 1-8, with maximum efficiencies occurring between TSR's of 3-5.<sup>6,7,9,15</sup> Thus, when

I began running simulations I ran them in these ranges of TSRs. The results, however were not TSR curves, but plots that increased exponentially in efficiency. A visual representation of this problem is shown in Figure 17. The same phenomena occurred at 8 and 9 m/s, plots of which, can be found in the Appendices.

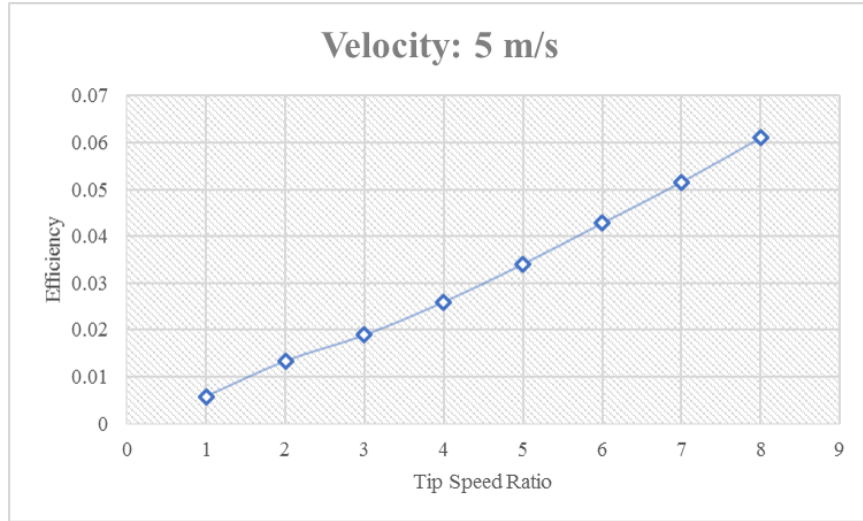


Figure 17: Exponentially Increasing Power Curve, 5 m/s

Another issue encountered, was that SimScale only permits 3000 hours of simulation time per community account. Once all the simulations were done I had run 5730 hours worth of simulations. Thus in the middle of the process I had to create a new account and replicate everything from the previous account to the new one.

## 4 Conclusions and Future Work

After running a variety of simulations on the wind turbine at various wind speeds and tip speed ratios, I have concluded that it is difficult, if not impossible to determine

the range of tip ratios that a wind turbine will operate at using SimScale. CFD software that is able to predict the rotational velocity and TSR based on a set wind speed would be exceptionally easier to use. SimScale's community plan is also not practical for large projects. In the future, software such as ANSYS could be purchased for increased capability and run-time.

Despite the difficulties faced determining the range of TSR's, successful results were obtained. Mesh convergence between  $10^{-4}$  and  $10^{-6}$ ,  $y+$  values under 200, and similar results between the simulation of the wind turbine at 12 m/s and the actual wind tunnel test data, were all found. Thus, the output of this simulation can be deemed accurate.

Future work could include running 3D simulations, which could provide increased accuracy in efficiency prediction. Another step could be to simulate the wind turbine in unsteady, time dependent simulations using the Arbitrary Mesh Interface SimScale option for rotational analysis. This method is more computationally expensive, however it takes into account the time-dependant nature of wind turbine simulation by physically rotating the geometry and extrapolating data at each time-step.<sup>13</sup>

A big issue encountered in both the simulations and the wind tunnel test was that the efficiency of the wind turbine was found to be unexpected low, and also runs at very low tip speed ratios. While research has shown that Gorlov style turbines are capable of having efficiencies as high as 30%, this turbine is only functioning at an efficiencies lower than 1%.

Future work could include continued corroboration with Dr. Tan to alter the wind turbine geometry to improve its' efficiency. The effects of altering pitch angle, airfoil style, height to diameter ratio, or other geometrical changes could be studied in with CFD. By creating new SolidWorks models, various geometries can be tested to determine the optimal shape of the wind turbine. The use of CFD can eliminate the “guess and check” work of altering the physical wind turbine, testing it in the wind tunnel, and and altering it again. This will save money, time, and material waste.

## **5 Acknowledgements**

I would like to acknowledge the 2013-2014 UVM senior design team who built the wind turbine used in this study, and the members of my 2016-2017 senior design team for completing the wind tunnel test and tabulating the results necessary for comparison. I would specifically like to thank Tommy Leger for creating the power coefficient plot of the wind turbine (Figure 9), and Benedict Delahunty for his help in the beginning stages of simulation and Solidwork design. I would also like to thank Dr. Yves Dubief and Dr. Ting Tan for their advice throughout this project.

## References

- [1] Rao, K. Murali Mohan, and K. Mohana Rao. "Extraction and tensile properties of natural fibers: Vakka, date and bamboo." *Composite structures* 77.3 (2007): 288-295.
- [2] Cengel, Yunus A.; Cimbala, John M., *Fluid Mechanics: Fundamentals and Applications*, 3rd ed., New York, New York (2014)
- [3] Sanderse, Benjamin, S. P. Pijl, and B. Koren. "Review of computational fluid dynamics for wind turbine wake aerodynamics." *Wind energy* 14.7 (2011): 799-819.
- [4] Chowdhury, Abdullah Mobin, Hiromichi Akimoto, and Yutaka Hara. "Comparative CFD analysis of vertical axis wind turbine in upright and tilted configuration." *Renewable Energy* 85 (2016): 327-337.
- [5] Rocha, PA Costa, et al. "A case study on the calibration of the k- SST (shear stress transport) turbulence model for small scale wind turbines designed with cambered and symmetrical airfoils." *Energy* 97 (2016): 144-150.
- [6] Balduzzi, Francesco, et al. "Dimensionless numbers for the assessment of mesh and timestep requirements in CFD simulations of Darrieus wind turbines." *Energy* 97 (2016): 246-261.
- [7] Gosselin, Rémi, Guy Dumas, and Matthieu Boudreau. "Parametric study of H-Darrieus vertical-axis turbines using uRANS simulations." 21st annual conference of the CFD society of Canada. 2013.
- [8] "FLUENT 6.1 Documentation." Fluent Incorporated, 25 Jan. 2003. Web. 15 Feb. 2017.
- [9] Bachant, Peter, and Martin Wosnik. "Modeling the near-wake of a vertical-axis cross-flow turbine with 2-D and 3-D RANS." *Journal of Renewable and Sustainable Energy* 8.5 (2016): 053311.
- [10] Lindblad, Daniel, Adam Jareteg, and Olivier Petit. "Implementation and runtime mesh refinement for the k- SST DES turbulence model when applied to airfoils." (2014).

- [11] Gulbe, Linda, Normunds Jekabsons, and Agris Traskovs. "Parametric Studies for Vertical Axis Wind Turbine Simulations." *Scientific Journal of Riga Technical University. Environmental and Climate Technologies* 6.1 (2011): 23-30.
- [12] Rocha, PA Costa, et al. "A case study on the calibration of the k- SST (shear stress transport) turbulence model for small scale wind turbines designed with cambered and symmetrical airfoils." *Energy* 97 (2016): 144-150.
- [13] "Rotating Zones." *SimScale Documentation*. Simscale, Web. 22 Apr. 2017.
- [14] ARIFF, Mohd, and Salim SALIM. "Wall Y+ Approach for Dealing With Turbulent Flow Over A Surface Mounted Cube: Part 1 – Low Reynolds Number." *Computational Fluid Dynamics. Seventh International Conference on CFD in the Minerals and Process Industries*, Dec. 2009. Web. 12 Apr. 2017.
- [15] Kulkarni, Siddharth Suhas, Craig Chapman, and Hanifa Shah. "Computational Fluid Dynamics (CFD) Mesh Independency Study of A Straight Blade Horizontal Axis Tidal Turbine." (2016).
- [16] Gorban, Alexander N., Alexander M. Gorlov, and Valentin M. Silantyev. "Limits of the turbine efficiency for free fluid flow." *Journal of energy resources technology* 123.4 (2001): 311-317.
- [17] "Navier Stokes Equations." *National Aeronautics and Space Administration. Glenn Research Center*, n.d. Web. 24 Apr. 2017.

## 6 Appendices

### 6.1 Exponentially Increasing Power Coefficient Curves

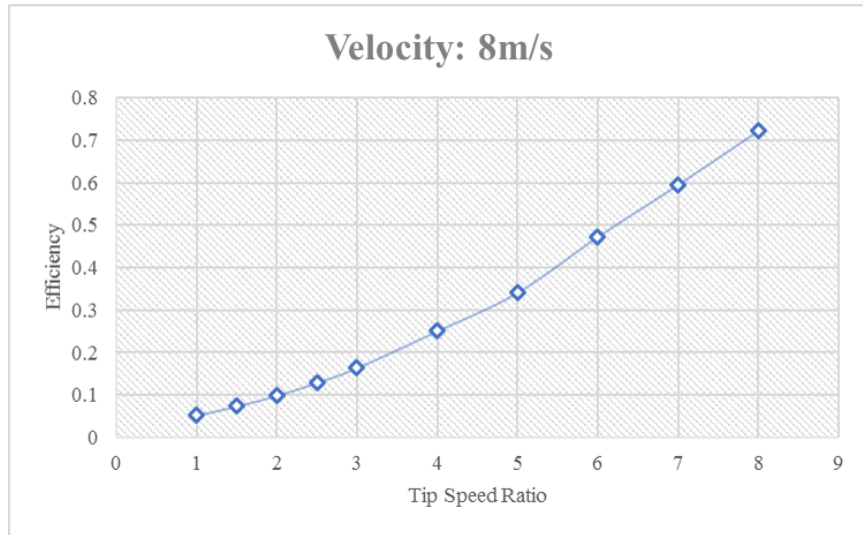


Figure 18: Exponentially Increasing Power Curve, 8 m/s

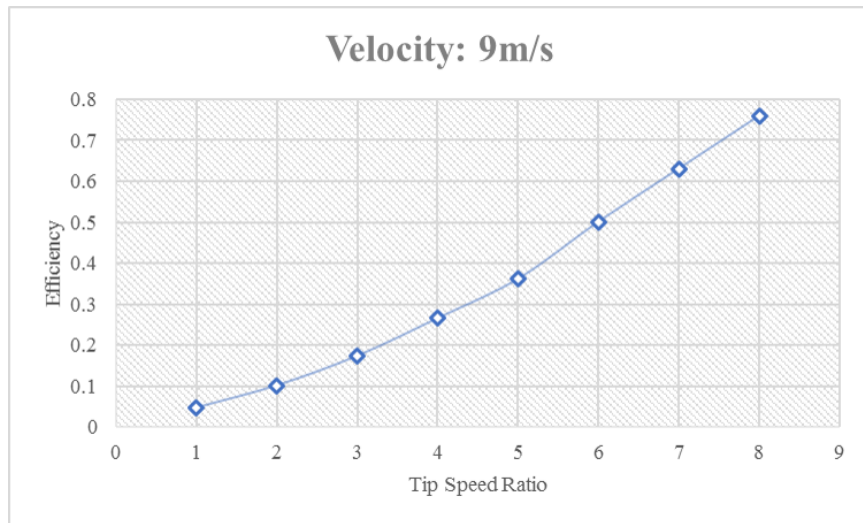


Figure 19: Exponentially Increasing Power Curve, 9 m/s

## 6.2 Convergence Plots

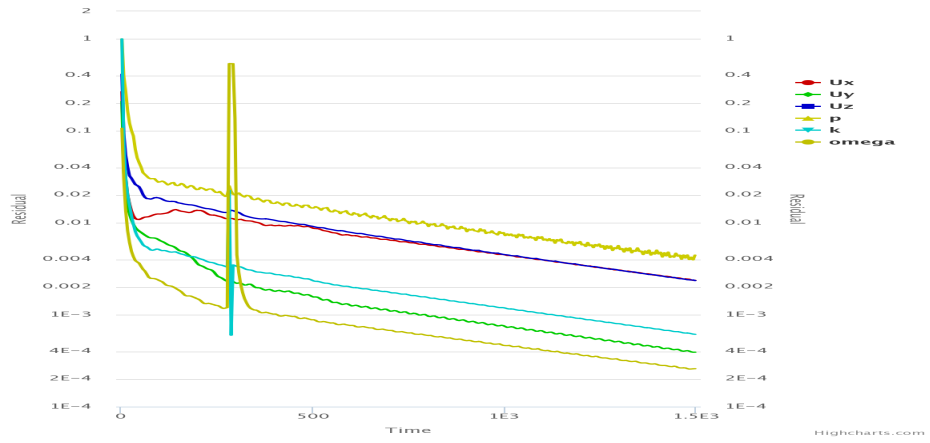


Figure 20: Convergence Plot, 5 m/s, TSR=3

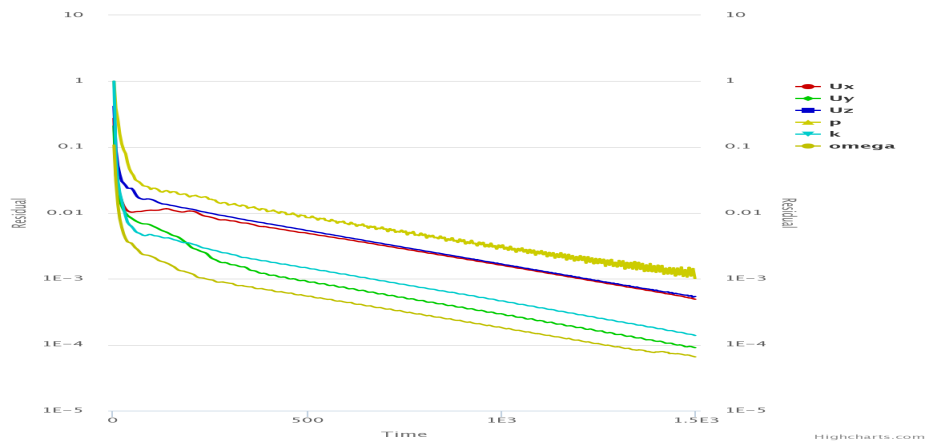


Figure 21: Convergence Plot, 5 m/s, TSR=4



### 6.3 Mesh Attempts

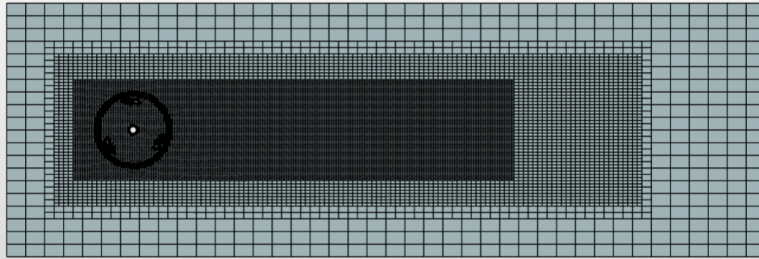


Figure 22: Mesh Attempt 1

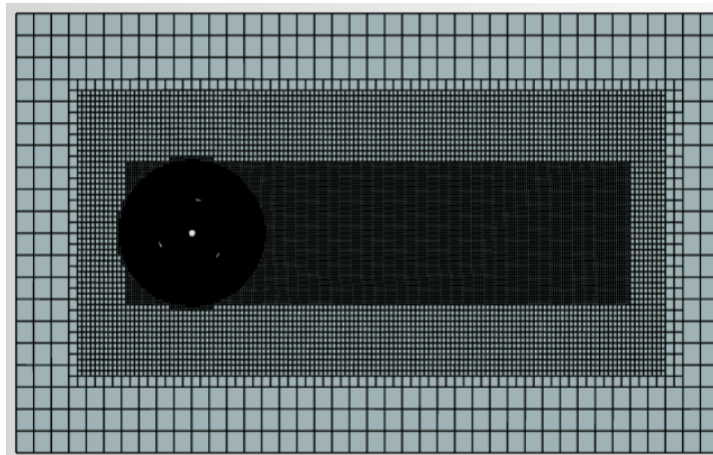


Figure 23: Mesh Attempt 2

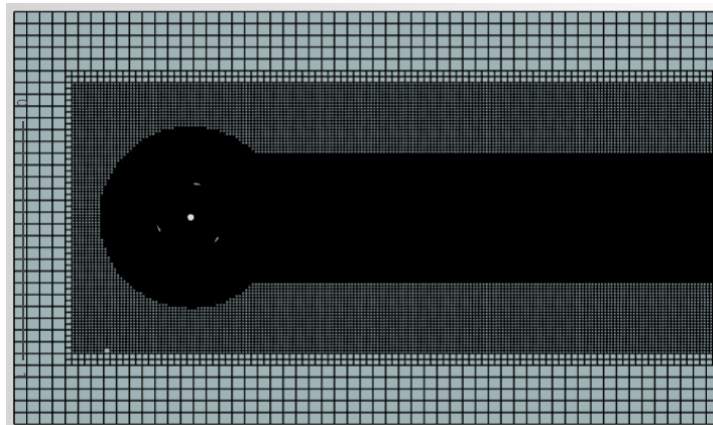


Figure 24: Mesh Attempt 3